

A radial velocity survey of low Galactic latitude structures: II. The Monoceros Ring behind the Canis Major dwarf galaxy

Blair C. Conn¹, Nicolas F. Martin^{2,4}, Geraint F. Lewis¹, Rodrigo A. Ibata², Michele Bellazzini³ & Mike J. Irwin⁴

¹Institute of Astronomy, School of Physics, A29, University of Sydney, NSW 2006, Australia:

Email bconn@physics.usyd.edu.au, gfl@physics.usyd.edu.au

²Observatoire de Strasbourg, 11, rue de l'Université, F-67000, Strasbourg, France:

Email ibata@astro.u-strasbg.fr, martin@astro.u-strasbg.fr

³INAF - Osservatorio Astronomico di Bologna, Via Ranzani 1, 40127, Bologna, Italy:

Email michele.bellazzini@bo.astro.it

⁴Institute of Astronomy, Madingley Road, Cambridge, CB3 0HA, U.K.:

Email mike@ast.cam.ac.uk

5 February 2008

ABSTRACT

An AAT/2dF Spectrograph Survey of low Galactic latitudes targeting the putative Canis Major dwarf galaxy, and the (possibly) associated tidal debris of stars known as the Monoceros Ring, covering Galactic coordinates $231.5^\circ < l < 247.5^\circ$ and $-11.8^\circ < b < -3.8^\circ$, has revealed the presence of the Monoceros Ring in the background of the Canis Major dwarf galaxy. This detection resides at a galactocentric distance of $\sim 18.9 \pm 0.3$ kpc (13.5 ± 0.3 kpc heliocentric), exhibiting a velocity of $\sim 132.8 \pm 1.3$ km s⁻¹ with a dispersion of $\sim 22.7 \pm 1.7$ km s⁻¹; both of these comparable with previous measurements of the Monoceros Ring in nearby fields. This detection highlights the increasing complexity of structure being revealed in recent surveys of the Milky Way thick disk and Halo.

Key words: Galaxy: structure – Galaxy: formation – galaxies: interactions

1 INTRODUCTION

Galaxy formation based on a Λ CDM cosmology predicts larger structures being formed from the accumulation of smaller systems (e.g. Searle & Zinn 1978; White & Rees 1978; White 1978; Abadi, Navarro, Steinmetz, & Eke 2003a,b). One of the core outcomes of this model is that the halos of galaxies should be strewn with the debris from all these minor mergers. The first discovery of such a merger within our own Milky Way, the Sagittarius dwarf galaxy (Ibata, Gilmore, & Irwin 1994), demonstrated that such mergers do occur and are in fact ongoing.

Insight into the complex nature of the Galactic Halo has been in part accomplished by recent all sky surveys, Sloan Digital Sky Survey (SDSS) and the Two Micron All Sky Survey (2MASS). Investigating an overdensity of F-turnoff stars in the SDSS, Newberg et al. (2002) discovered the presence of a stream of stars suggestive of an equatorial accretion event around the Milky Way. Unlike the Sagittarius dwarf galaxy which is on a polar orbit, this accretion event may have implications on the formation of key Galactic structures, such as the thick disk. The equatorial orbit of the stream was investigated by Crane et al. (2003) who targeted 2MASS selected M-giant stars in the range $l = 150^\circ - 240^\circ$, although primarily in the Northern hemisphere, finding that a simple circular orbit model with a galactocentric radius of 18 kpc and

velocity of ~ 220 km s⁻¹ best fit the data. The velocity dispersion of their sample was 20 ± 4 km s⁻¹ which excludes it from being of Galactic origins. As more detections of this structure were made (Yanny et al. 2004; Ibata et al. 2003; Rocha-Pinto et al. 2003) it became clear that, as proposed by Newberg et al. (2002), this was indeed another on-going accretion event. The search for the progenitor of the stream in the 2MASS catalog led Martin et al. (2004a) to uncover the Canis Major dwarf galaxy ($l, b = \sim(240^\circ, -8^\circ)$).

Because of the low density of stream material on the sky it has been necessary to employ the use of Wide-Field Cameras to look deeply into Milky Way's thick disk and Halo, not only confirming and enhancing previous detections but probing new regions leading to more detections of the Monoceros Ring and the Canis Major dwarf being made (Martin et al. 2004a; Bellazzini et al. 2004; Conn et al. 2005; Martínez-Delgado et al. 2005). Detections of an additional structure in Triangulum-Andromedae (Rocha-Pinto et al. 2004; Majewski et al. 2004) are revealing the increasing complexity of accretion events in the outer regions of the Galaxy. Current debate on these detections centres on whether these represent separate accretion events or are the product of a single ongoing merger. The location of the progenitor is still contentious but this paper will refer to the Canis Major overdensity as the Canis Major dwarf galaxy (CMa), following the conclusions of Martínez-Delgado et al. (2005) and Martin et al. (2005a).

While the positions of the streams on the sky are highly accurate, the distance estimates to the stars are less so, requiring the need for radial velocity kinematic measurements to increase and characterize the known properties of the streams. Distances are then estimated through photometric parallaxes as described in Martin et al. (2004b). To date, several kinematic surveys of the Monoceros Stream have been undertaken using the data of 2MASS and SDSS (Yanny et al. 2004; Crane et al. 2003; Rocha-Pinto et al. 2004). These have confirmed a velocity gradient with Galactic longitude and also a low velocity dispersion of $\sigma_{(v_r)} \sim 20 \text{ km s}^{-1}$ for the Monoceros Ring.

While most models of equatorial accretion onto disk-like galaxies (e.g. Peñarrubia et al. 2005; Martin et al. 2005a) predict the presence of multiply wrapped streams, no detections provide conclusive evidence supporting this hypothesis. This is most likely due to the pencil beam nature of most fields with regard the entire structure on the sky and given that confirmed detections of the stream are limited to galactic longitudes ($120^\circ < l < 240^\circ$) and significant areas of this structure are yet to be sampled. This new detection presented here is consistent with multiply wrapped streams.

2 OBSERVATIONS AND REDUCTION

In April 2004, a survey was undertaken with the 2dF (Two-degree Field) multi-fibre spectrograph on the Anglo-Australian Telescope (AAT) with two aims: firstly, to determine the kinematics of the Canis Major dwarf, and secondly to try and locate the stars belonging to the Monoceros Ring through kinematic constraints. Out of ~ 15 fields, eight were dedicated to this purpose, four focusing solely on the Canis Major region. This paper will focus primarily on results pertaining to the detection of the Monoceros Ring in the Canis Major dwarf region, the same area studied by Martin et al. (2005a); hereafter Paper I.

The 2dF instrument is capable of measuring velocities of ~ 400 stars simultaneously within a two degree field of view. The field is divided between two spectrographs, the first using a 1200V grating (4600-5600Å at 1Å/pixel); the second using a 1200R grating (8000-9000Å at 1Å/pixel). The configuration on the second spectrograph was chosen to target Red Clump stars in the distance range 5-8 kpc, these stars fall outside the distance range expected for the Monoceros Ring and thus are not discussed in this paper. (Paper I discusses the results of the survey in the region < 10 kpc.)

The Red Giant Branch (RGB) stars in this survey were chosen from Sample A of Martin et al. (2004a). Using the photometric parallax technique of Majewski, Skrutskie, Weinberg, & Ostheimer (2003) to determine the distances, the stars in the correct distance range for the Monoceros Ring can then be easily selected. Determining the exact error on the distance using this technique is difficult and so for these observations a conservative estimate of ± 1 kpc for these stars has been assumed. The J,H,K magnitudes from the 2MASS catalogue for these stars have been de-reddened using the dust maps of Schlegel, Finkbeiner, & Davis (1998) and the asymptotic correction of Bonifacio et al. (2000).

2.1 Reducing 2dF spectra

Data reduction of the 2dF spectra involves using the 2dFDR package (Taylor et al. 1996) which applies the flat field correction, sky subtraction and extracts the individual spectra from each fibre off the CCD. Due to an asymmetry in the Line Spread Function (LSF)

of the spectra a *custom-made* reduction pipeline was constructed to minimise the errors this produced when comparing with radial velocity standard stars; a detailed presentation of the pipeline can be found in Martin et al. (2005b). This pipeline limits the systematic offsets in the radial velocity due to the LSF to $\pm 5 \text{ km s}^{-1}$, this value is not included in the errors stated. Determining the radial velocities, v_r , using several artificial standard star templates and taking a weighted average of the solutions avoids any systematic offset that may result from a peculiarity in one of the templates (Martin et al. 2005a,b). Stars then with $\sigma_v > 5 \text{ km s}^{-1}$ (See Equation 2 of Paper I) are removed from the sample to avoid contaminating the results with poor determination of radial velocity. Dust extinction in this region typically is $E(B-V) < 0.4$ (taken from Schlegel, Finkbeiner, & Davis 1998) and only the field closest to the plane has higher extinction. There has been no significant impact on the 2MASS colours due to extinction.

2.2 Determining the Fit and the Associated Error

For each velocity and distance distribution, a Gaussian has been fitted to the profile using an amoeba routine (Press et al. 1992), obtaining a characteristic velocity, velocity dispersion, distance and distance dispersion which best represents the data. The errors on the fitted parameters were determined by bootstrap re-sampling and then refitting the data. The re-sampling was undertaken using the errors of each quantity namely the conservative ± 1 kpc for the distance to each star and the root-mean-square value of the dispersion. The errors cited then, are the standard deviations of the fit determined using this method. There is no appreciable difference between the galactocentric and heliocentric errors in this field. The velocity errors also have an additional $\pm 5 \text{ km s}^{-1}$ systematic error on top of the stated errors.

3 RESULTS

3.1 The Monoceros Ring behind the Canis Major dwarf

The data in Figure 1 was taken from six fields of the 2dF spectrographic survey and shows a population of ~ 38 RGB stars behind the Canis Major overdensity. These stars are represented in the solid histogram while the dashed histogram is the remaining stars in that region. The stars have been selected using the following criteria, $231.5^\circ < l < 247.5^\circ$ and $-11.8^\circ < b < -3.8^\circ$; $12 \text{ kpc} < D_\odot < 20 \text{ kpc}$ and a colour cut of $0.9 < (J-K)_o < 1.3$; $0.561(J-K)_o + 0.22 < (J-H)_o < 0.561(J-K)_o + 0.36$; $K_o \leqslant 13.0$; with $v_r > 0 \text{ km s}^{-1}$. This overdensity shows up very clearly in the galactocentric distance histogram and given the distance range of these stars makes them different from the foreground Canis Major stars as presented in Paper I. They form a coherent velocity and distance structure similar to that of previous Monoceros Ring detections. Figure 1 shows the 2dF Data with a Gaussian fit of $v_r = 132.8 \pm 1.3 \text{ km s}^{-1}$ and internal dispersion of $22.7 \pm 1.7 \text{ km s}^{-1}$, which is comparable to the dispersion as measured by Yanny et al. (2004) from SDSS data. The galactocentric distance estimates to this feature are 18.9 ± 0.3 kpc with a dispersion of 0.8 ± 0.4 kpc. See §2.2 or Paper I for a more complete breakdown on the errors, however note again that the errors have an additional systematic offset of $\pm 5 \text{ km s}^{-1}$. To test the contamination of local dwarfs which fall inside the selection criteria for the sample stars due to poor extinction correction, the data has been tested with a more stringent cutoff of $(J-K)_o > 0.95$. This still

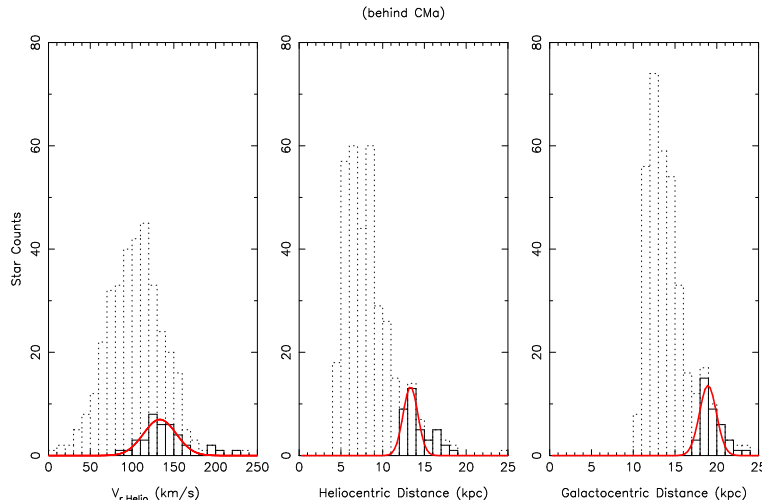


Figure 1. Histogram of the 2dF RGB data in the range $231.5^\circ < l < 247.5^\circ$ and $-11.8^\circ < b < -3.8^\circ$; with a heliocentric distance cut of $12 \text{ kpc} < D_\odot < 20 \text{ kpc}$ and the following additional cuts of $0.9 < (J-K)_0 < 1.3$; $0.561(J-K)_0 + 0.22 < (J-H)_0 < 0.561(J-K)_0 + 0.36$; $K_0 \leqslant 13.0$ and $v_r > 0 \text{ km s}^{-1}$. This field constitutes the region behind the Canis Major overdensity revealing a detection of the Monoceros Ring at a galactocentric distance of $18.9 \pm 0.3 \text{ kpc}$ and a dispersion of $0.8 \pm 0.4 \text{ kpc}$ (right panel) with a heliocentric distance of $13.5 \pm 0.3 \text{ kpc}$ with similar dispersion (middle panel). The velocity profile fitted to this population is $v_r = 132.8 \pm 1.3 \text{ km s}^{-1}$ with an internal dispersion of $22.7 \pm 1.7 \text{ km s}^{-1}$ (left panel), the error is accompanied by an additional systematic offset of $\pm 5 \text{ km s}^{-1}$. The dashed lines shows the remaining data outside the distance and colour cut. For a full outline of the errors see §2.2 and Paper I.

reproduces the detection presented here suggesting the contamination level is low.

Although, as can be seen in Figure 1, there is no definitive evidence for a *gap* between the Canis Major detection and the Monoceros Ring detection this is most likely due to the large errors in the distance rather than the structure being somewhat continuous out to large galactocentric distances. The conservatively estimated error on the distance is $\sim 1 \text{ kpc}$, which will have the effect of blurring any intrinsic gap between the two structures. Contamination from local dwarfs although believed to be minimal will also impact on the ability to resolve the stream out cleanly from the Canis Major population. It should also be noted that depending on the formation scenario of the stream the stars may or may not be neatly confined at one distance but rather diffused over a larger volume. Since the origins and evolution of both structures is still being investigated, explaining the lack of a gap in distance is at best speculative. With these stars being selected from the 2MASS catalogue a measure of the completeness of the sample becomes possible. Applying the colour cuts used on the 2dF data to the 2MASS catalogue reveals 399 stars in this region of which 364 have been observed making this sample $\sim 91\%$ complete.

In Paper I, a northern comparison field at $(240.0^\circ, +8.8^\circ)$ is presented for the Canis Major detection. Unfortunately, the number of RGB stars sampled out to large Galactic radii is too low to form a useful comparison with the detection presented in this paper.

3.2 The Besançon Synthetic Galaxy Model

Understanding what the Galactic contribution is in any given region of sky is critical when attempting to interpret the results of this 2dF survey. To investigate this, the synthetic galaxy model of Robin, Reylé, Derrière & Picaud (2003) is used to find out what the model predicts our Galactic contamination should be. This is done by selecting the exact same regions of sky as observed in the 2dF survey. Given the tight constraints in colour and magnitude used to select the stars in our survey (see Paper I) applying the same constraints to the synthetic Galaxy model to provide an idea of the

contamination we should expect was undertaken. In particular these are: $0.9 < (J-K)_0 < 1.3$; $0.561(J-K)_0 + 0.22 < (J-H)_0 < 0.561(J-K)_0 + 0.36$; $K_0 \leqslant 13.0$; $v_r > 0 \text{ km s}^{-1}$. The cuts were applied to the model which extended to a heliocentric distance of 100 kpc.

To remove the presence of noise in the model, each field was investigated using the online model selecting the *small field* setting with a solid angle of 1000 deg^2 . This has the effect of providing a smoother distribution of the stars with the properties determined by the centre of the field, rather than the *large field* option which takes into account changes in $(l, b)^\circ$. Each field is then rescaled back to the size of the 2dF fields and rescaled to match the completeness of the 2dF sample with regard the 2MASS catalogue. These stars are presented in Figure 2 and in general have a much broader distribution than could be attributed to any tidal debris with velocities which typically peak well away from the 2dF detections. As expected, in the distance range of the MRI there is no thin disk population and with the thick disk only having ~ 15 stars in this location; halo stars are expected to only have a very small presence in this field and are not included in these results. The comparisons with the Besançon model provide good support for the validity of this detection with the usual precautions.

The approximately 15 stars which fall in the region of the MRI in the model have the following properties, a velocity profile of $v_r = 143.8 \text{ km s}^{-1}$ and dispersion of 28.2 km s^{-1} ; galactocentric distance profile of 19.7 kpc with a dispersion of 1.9 kpc . A Kolmogorov-Smirnov test of the MRI stars from the 2dF sample and the Besançon stars finds a 4% chance of the two being drawn from the same distribution. This is a relatively high probability of coincidence however a few extra factors need to be taken into account. While the model contains thick disk stars with an additional warp component, the data contains thick disk stars, CMa stars and MRI stars with a warp component mixed in. What effect does this have on our comparison? Since a completeness factor has been derived from the 2MASS catalogue and subsequently used to scale the Besançon model and given the 2MASS stars contains a significant proportion of CMa stars then the numbers of thick disk stars must be being overestimated. This has the immediate effect of low-

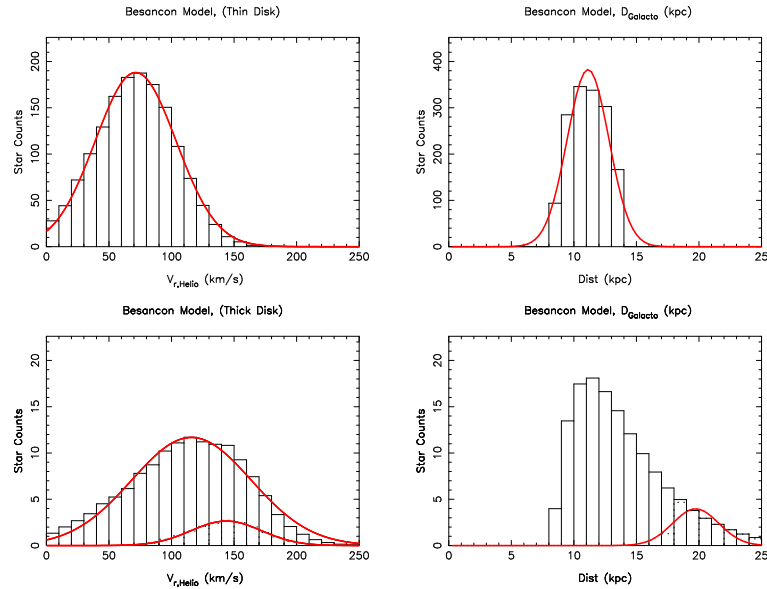


Figure 2. Histogram of Besançon data covering the same region of sky as the 2dF dataset; no distance cuts have been applied less than the 100 kpc cutoff of the model. The distances are galactocentric to allow easy comparison with the 2dF data as shown in Figure 1. The top panels show the thin disk population (stars in the age range 5-7 Gyrs) in this field fitted with a Gaussian profile at a distance of ~ 11.1 kpc and a dispersion of ~ 1.7 kpc. The velocity profile of the thin disk stars is $v_r = \sim 71.4$ km s $^{-1}$ with a dispersion of ~ 32.3 km s $^{-1}$. In the bottom panels are the thick disk stars (noting that these stars have a different density profile than the thin disk stars) they too can be fitted with a Gaussian profile and reside at a galactocentric distance of 13.1 kpc with a dispersion of 5.0 kpc, the velocity and dispersion are found to be $v_r = 115.9$ km s $^{-1}$ and 47.7 km s $^{-1}$ respectively. The smaller Gaussians represent those 15 stars in the same distance range as the MRI stars in Figure 1 with $v_r = 143.8$ km s $^{-1}$ and a dispersion of 28.2 km s $^{-1}$; galactocentric distance of 19.7 kpc with a dispersion of 1.9 kpc.

ering the number of stars that can be expected in the distance range of the MRI. The true number of Galactic thick disk stars would be much less than the ~ 15 stars presented in Figure 2, especially since most of the stars as presented in Paper I seem to belong to the CMa structure and that confusion over whether they represent the warp seems to have been sufficiently discounted.

4 DISCUSSION & CONCLUSION

Comparisons with the Besançon synthetic galaxy model (Figure 2) reveal that the peak velocity and dispersion observed in this field cannot be associated with any known Galactic component. The thick disk component in the same region as the MRI has a higher velocity and a broader velocity dispersion which discounts it as the cause of the overdensity measured in this field (see Figure 1). This is supported by the finding that the numbers of thick disk stars in the model are being overestimated (after scaling) due to the presence of the CMa structure boosting the numbers of stars in the region. Although difficult to quantify it is expected that the numbers of Galactic thick disk stars should be much less than the ~ 15 stars as currently predicted. Investigating any similarities with previous detections of the Monoceros Ring finds encouraging agreement in the velocity dispersion estimates of Yanny et al. (2004) and Crane et al. (2003), which have values of 13 - 24 km s $^{-1}$ and 20 ± 4 km s $^{-1}$, respectively compared to 22.7 ± 1.7 km s $^{-1}$ from this paper.

The best model of the MRI with which to compare our detection is the Crane et al. (2003) circular orbit model since we target similar stars (M giant stars extracted from 2MASS) and since they reach a Galactic longitude of $l \sim 220$ in the Southern hemisphere and $l \sim 240$ degrees in the Northern hemisphere. Moreover, as has already been noticed, the velocity dispersion of our sample ($\sigma =$

22.7 ± 1.7 km s $^{-1}$) is statistically similar to the Crane et al. (2003) value (20 ± 4 km s $^{-1}$). It can be seen on Figure 3, where our targets are plotted as filled circles, that the velocity of our sample is only slightly higher than that expected by the circular model. Such a small discrepancy is not unexpected since the MRI population certainly does not follow a perfectly circular orbit (as is hinted by detections at different galactocentric distances within the $14 < D_{GC} < 20$ kpc distance range). Moreover, a closer look at Figure 2 of Crane et al. (2003) reveals the stars at high longitude in their sample ($l > \sim 220$ deg) also tend to have a radial velocity 20-30 km s $^{-1}$ higher than the circular orbit model. Thus, our detection of the Monoceros Ring is consistent with the current knowledge of this outer disk structure.

Equatorial accretion models predict the presence of wrapped tidal arms and this detection provides a tentative confirmation of such a scenario. A plausible alternative is that both the foreground Canis Major detection and the background Monoceros Ring detection represent separate accretion events. However, such a situation complicates the picture with the requirement of two progenitor systems hidden somewhere in the Milky Way. Hence, we conclude that the probable scenario is that the Canis Major dwarf and the Monoceros Ring represent a single accretion event and this new detection is of a wrapped tidal arm.

5 ACKNOWLEDGEMENTS

BCC's thanks go to the Anglo-Australian Observatory and the ANU Lodge for the technical support and hospitality received during his stay. GFL acknowledges the support of the Discovery Project grant DP0343508 and would like to thank Little Britain and Trish, you know Trish... Trish Trish, well anyway she's got nuffin to do wiv it, so Shyap! NFM acknowledges support from a

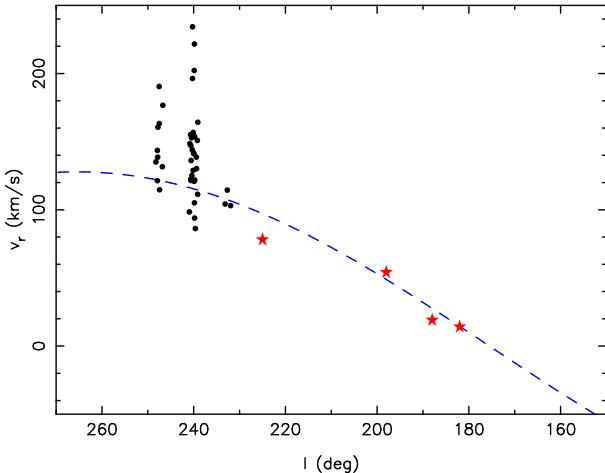


Figure 3. Distribution of the target M giant stars compared to previous detections of the MRI. Stars from our sample are shown as filled circles whereas SDSS detections are plotted as stars. The dashed line corresponds to the best circular orbit model from Crane et al. (2003) for a population orbiting the Milky Way at $D_{GC}=18$ kpc with a rotational velocity of $v_{rot}=220$ km s $^{-1}$

Marie Curie Early Stage Research Training Fellowship under contract MEST-CT-2004-504604.

REFERENCES

- Abadi, M. G., Navarro, J. F., Steinmetz, M., & Eke, V. R. 2003a, ApJ, 597, 21
 Abadi, M. G., Navarro, J. F., Steinmetz, M., & Eke, V. R. 2003b, ApJ, 591, 499
 Bellazzini, M., Ibata, R., Monaco, L., Martin, N., Irwin, M. J., & Lewis, G. F. 2004, MNRAS, 354, 1263
 Bonifacio, P., Monai, S., & Beers, T. C. 2000, AJ, 120, 2065
 Conn, B. C., Lewis G. F., Irwin M. J., Ibata, R. A., Irwin J. M., Ferguson, A. M. N. & Tanvir, N. R. 2005, MNRAS, accepted, *astro-ph/0506522*
 Crane J. D., Majewski S. R., Rocha-Pinto H. J., Frinchaboy P. M., Skrutskie M. F. & Law D. R. 2003, ApJ, 594, L119
 Ibata, R. A., Gilmore, G., & Irwin, M. J. 1994, Nature, 370, 194
 Ibata R. A., Irwin M. J., Lewis G. F., Ferguson A. M. N. & Tanvir N. 2003, MNRAS, 340, L21
 Majewski, S. R., Skrutskie, M. F., Weinberg, M. D., & Ostheimer, J. C. 2003, ApJ, 599, 1082
 Majewski, S. R., Ostheimer, J. C., Rocha-Pinto, H. J., Patterson, R. J., Guhathakurta, P., & Reitzel, D. 2004, ApJ, 615, 738
 Martin, N. F., Ibata, R. A., Bellazzini, M., Irwin, M. J., Lewis, G. F. & Dehnen, W. 2004a, MNRAS, 348, 12
 Martin, N. F., Ibata, R. A., Conn, B. C., Lewis, G. F., Bellazzini, M., Irwin, M. J., & McConnachie, A. W. 2004b, MNRAS, 355, L33
 Martin, N. F., Ibata, R. A., Conn, B. C., Lewis, G. F., Bellazzini M. & Irwin, M. J. 2005a, MNRAS, in press, *astro-ph/0503705*, (Paper I)
 Martin, N. F., Ibata, R. A., Conn, B. C., Irwin, M. J. & Lewis, G. F. 2005b, PASA, submitted
 Martínez-Delgado, D., Peñarrubia J., Dinescu, D. I., Butler, D. J., Rix H.W. 2005, in press, *astro-ph/0506012*
 Newberg H. J. et al. 2002, ApJ, 569, 245
 Peñarrubia, J., et al. 2005, ApJ, 626, 128
 Press, W. H., Teukolsky, S. A., Vetterling, W. T., & Flannery, B. P. 1992, Cambridge: University Press, —c1992, 2nd ed.,
 Robin, A. C., Reylé, C., Derrière, S. & Picaud, S. 2003, A&A, 409, 523
 Rocha-Pinto, H. J., Majewski, S. R., Skrutskie, M. F., Crane, J. D., & Patterson, R. J. 2004, ApJ, 615, 732
 Rocha-Pinto H. J., Majewski S. R., Skrutskie M. F. & Crane J. D. 2003, ApJ, 594, L115
 Schlegel D. J., Finkbeiner D. P. & Davis M. 1998, ApJ, 500, 525
 Searle, L. & Zinn, R. 1978, ApJ, 225, 357
 Taylor, K., Bailey, J., Wilkins, T., Shortridge, K., & Glazebrook, K. 1996, ASP Conf. Ser. 101: Astronomical Data Analysis Software and Systems V, 101, 195
 White, S. D. M. 1978, MNRAS, 184, 185
 White, S. D. M. & Rees, M. J. 1978, MNRAS, 183, 341
 Yanny B., et al., 2004, ApJ, 605, 575